Development 134, 1051-1060 (2007) doi:10.1242/dev.02817

Redundancy and specialization among plant microRNAs: role of the *MIR164* family in developmental robustness

Patrick Sieber[1,2], Frank Wellmer[1], Jacqueline Gheyselinck[2], José Luis Riechmann[1] and Elliot M. Meyerowitz[1,*]

In plants, members of microRNA (miRNA) families are often predicted to target the same or overlapping sets of genes. It has thus been hypothesized that these miRNAs may act in a functionally redundant manner. This hypothesis is tested here by studying the effects of elimination of all three members of the *MIR164* family from *Arabidopsis*. It was found that a loss of *miR164* activity leads to a severe disruption of shoot development, in contrast to the effect of mutation in any single *MIR164* gene. This indicates that these miRNAs are indeed functionally redundant. Differences in the expression patterns of the individual *MIR164* genes imply, however, that redundancy among them is not complete, and that these miRNAs show functional specialization. Furthermore, the results of molecular and genetic analyses of *miR164*-mediated target regulation indicate that *miR164* miRNAs function to control the transcript levels, as well as the expression patterns, of their targets, suggesting that they might contribute to developmental robustness. For two of the *miR164* targets, namely *CUP-SHAPED COTYLEDON1* (*CUC1*) and *CUC2*, we provide evidence for their involvement in the regulation of growth and show that their derepression in *miR164* loss-of-function mutants is likely to account for most of the mutant phenotype.

KEY WORDS: MicroRNA, *miR164*, Organogenesis, Developmental robustness, Phyllotaxis, *CUP-SHAPED COTYLEDON*

INTRODUCTION

MicroRNAs (miRNAs) are short (~21 nucleotide) non-translated RNAs that are generated by the enzymatic processing of stem-loop regions of longer precursor RNAs (Bartel, 2004; Valencia-Sanchez et al., 2006; Vaucheret, 2006). miRNAs are present in both plants and animals, and they regulate gene expression in a sequence-specific manner by targeting mRNAs for cleavage or translational repression. Animal miRNAs typically act by inhibiting translation of their targets, with which they usually share relatively low sequence complementarity (Lim et al., 2005). As a result, a given animal miRNA might target many different genes, and a large fraction of the animal transcriptome has been proposed to be directly influenced by miRNA control (Farh et al., 2005; Stark et al., 2005). By contrast, plant miRNAs use cleavage as the preferential mechanism for target gene regulation, they tend to exhibit a high degree of complementarity to their targets, and appear to have fewer target genes per miRNA (Llave et al., 2002; Schwab et al., 2005). The existence of perfect or nearly perfect complementarity between plant miRNAs and mRNAs has greatly facilitated the identification of putative targets for many of the characterized miRNAs (Rhoades et al., 2002). In *Arabidopsis*, 165 miRNA loci have been identified so far, which are grouped into 93 different miRNA families (Lu et al., 2006; Rajagopalan et al., 2006; Reinhart et al., 2002) (miRBase, release 9.0, http://microrna.sanger.ac.uk/). At least 70 of these miRNA loci, comprising 21 gene families, have been predicted or demonstrated to target genes encoding transcription factors. This prevalence of regulatory genes points to a central role for miRNAs in the control of gene regulatory networks in plants. Consistent with this notion, it has been shown that miRNAs are required in many developmental processes in plants, including organ polarity determination, meristem function, floral patterning, vascular development, lateral root development and hormone response (Baulcombe, 2004; Chen, 2005; Mallory and Vaucheret, 2006). The participation of miRNAs in these processes has been established primarily through their overexpression, or by generating plants that express miRNA-resistant versions of their target gene(s). By contrast, mutants have been isolated for only a few miRNAs (Aukerman and Sakai, 2003; Baker et al., 2005; Guo et al., 2005; Kim et al., 2005; Palatnik et al., 2003; Williams et al., 2005), and thus far only a single loss-of-function mutant for a plant miRNA has been identified in a forward genetic screen: the Arabidopsis *early extra petals1* mutant (*eep1*), in which *miR164c* function is disrupted (Baker et al., 2005).

The scarcity of identified loss-of-function mutants and phenotypes might be attributed to the fact that many miRNAs belong to multigene families, which are predicted to target the same (or overlapping) sets of genes, opening the possibility of substantial functional redundancy among miRNAs in plants. Although for *Caenorhabditis elegans* it has been shown that some members of the *let-7* family can have redundant functions (Abbott et al., 2005), evidence for redundancy among plant miRNAs has only been circumstantial. For example, loss of a single miRNA of a multigene family did not result in an aberrant phenotype in tissues where the miRNA was expressed (Mallory et al., 2004).

The *Arabidopsis MIR164* family comprises three members (*miR164a*, *miR164b* and *miR164c*) and negatively regulates, through mRNA cleavage, several genes that encode NAC-like transcription factors (Baker et al., 2005; Guo et al., 2005; Kasschau et al., 2003; Laufs et al., 2004; Mallory et al., 2004; Park et al., 2002). These genes include *CUP-SHAPED COTYLEDON1* (*CUC1*) and *CUC2*, which are expressed in, and are necessary for, the formation of boundaries between meristems and emerging organ primordia (Aida et al., 1999; Heisler et al., 2005; Takada et al., 2001). Failure to establish organ boundaries leads to severe developmental consequences, and in loss-of-function *cuc1 cuc2* double-mutant

[1]Division of Biology, California Institute of Technology, Pasadena, CA 91125, USA. [2]Institute of Plant Biology, University of Zurich, Zollikerstrasse 107, 8008 Zurich, Switzerland.

*Author for correspondence (e-mail: meyerow@its.caltech.edu)

Accepted 22 January 2007

seedlings the two cotyledons fail to separate and the seedling meristem arrests (Aida et al., 1997). Expression of miRNA cleavage-resistant versions of *CUC1* and *CUC2* in *Arabidopsis* has revealed that *miR164*-mediated repression of *CUC1* and *CUC2* is necessary for proper control of organ number (Baker et al., 2005; Mallory et al., 2004) and for organ boundary formation (Laufs et al., 2004). Analysis of *eep1* mutants has shown that *miR164c* functions to prevent extra petals in early-arising flowers by repressing *CUC1* and *CUC2* (Baker et al., 2005). The role of the *MIR164* family is not limited to flower development, however, as both *miR164a* and *miR164b* have been reported to prevent lateral root initiation by repressing the *miR164* target *NAC1* (Guo et al., 2005). In addition, ectopic expression of *miR164*-resistant versions of CUC1 and CUC2, respectively, was shown to lead to abnormal vegetative development (Laufs et al., 2004; Mallory et al., 2004; Nikovics et al., 2006). Taken together, these results suggest that *miR164* miRNAs may act throughout plant development.

Here, we report on the elimination of the activity of the entire *MIR164* family, and its consequences for development, demonstrating that all *miR164* miRNAs function redundantly during *Arabidopsis* shoot development, and uncovering new functions for these genes, including the regulation of phyllotaxis (the arrangement of organs along the stem) and developmental robustness.

MATERIALS AND METHODS

Plant material and growth conditions

Arabidopsis thaliana plants were grown as described previously (Baker et al., 2005). *mir164a-4* (this study) (Nikovics et al., 2006) and *mir164b-1* (Baker et al., 2005; Mallory et al., 2004) were isolated in the accession Columbia (Col-0). *eep1*, here referred to as *mir164c-1*, was isolated in Landsberg *erecta* (L*er*). Although *mir164c-1* mutants transcribe reduced amounts of *pri-miR164c*, they fail to effectively repress *CUC1* and *CUC2* function and thus may represent functionally null mutants (Baker et al., 2005). The *mir164c-2* allele (Col-0 background) represents a dSpm transposon insertion (dSpm_3_25571) 85 bp 3′ of the mature *miR164c* miRNA. Disruption of the predicted *pre-miR164c* stem loop in this allele does not cause any obvious mutant phenotype. In addition, *mir164a-4 b-1 c-2* triply homozygous mutant plants fail to show any increase in severity of their phenotype as compared with the respective single mutants (data not shown). The *mir164a-4* allele, isolated from the GABI-Kat collection (Rosso et al., 2003), was crossed to plants doubly homozygous for *mir164b-1* and *mir164c-1* (Baker et al., 2005). Progeny of three independent crosses (n_{tot}=246) were genotyped at all three *MIR164* loci (see below). Twelve plants were homozygous for all three *mir164* mutant alleles. *mir164a-4 b-1 c-1* triply homozygous plants always showed a novel phenotype, referred to as the *mir164abc* mutant phenotype. Floral organ counts were performed on 15 *mir164abc* triple mutants and 15 *mir164aAbBcC* 'wild-type' control plants, in both cases of a mixed L*er*/Col background. The *mir164abc* triple mutant was backcrossed once to Col-0 and to L*er* wild-type plants to assess potential contributions of either background to the phenotype.

Plasmid constructs

The *pCUC1::CUC1-GFP* and *pCUC1::CUC1^{m}-GFP* constructs have been described previously (Baker et al., 2005). *pCUC2::CUC2-GFP* was cloned by recombining DNA fragments essentially as described for *pCUC2::CUC2-VENUS-N7* (Heisler et al., 2005), except that mGFP5 was used as an alternative green fluorescent protein (GFP) instead of VENUS-N7. To generate *pCUC2::CUC2^{m}-GFP*, the *CUC2* coding region was mutated by exchanging nucleotides 772-792 (5′-GAGCACGTGT-CCTGTTTCTCC-3′) for 5′-GAACATGTATCATGCTTTAGC-3′ (base changes are underlined), thereby introducing eight silent mutations, which left the amino acid sequence of the CUC2 protein unchanged. Mutations were introduced by applying a PCR-mediated in vitro mutagenesis strategy as described for *pCUC1::CUC1^{m}-GFP* (Baker et al., 2005). The transcriptional reporter *pCUC1::3XVENUS-N7* was generated as follows: a 1.4 kb *Eco*RI-*Sfi*I fragment that contained the endogenous *CUC1* regulatory sequences (Baker et al., 2005) was blunt-ended using T4 DNA polymerase; this promoter fragment was subsequently introduced into the *Sma*I site of plasmid pPD35 (Heisler et al., 2005) (kindly provided by Dr P. Das) and the resulting plasmid was tested for the correct orientation of the insert. *pCUC2::3XVENUS-N7* has been previously described (Heisler et al., 2005). 1882 bp of *MIR164a* 5′ promoter sequence was amplified from Col-0 genomic DNA using the primer combination PS272/PS273 (Table 1). The *Nde*I-*Xho*I digested PCR fragment was cloned into the corresponding restriction sites of pPD35 to generate *pMIR164a::3XVENUS-N7*. The fragment corresponding to 2548 bp of *MIR164b* 5′ upstream sequence was cloned analogously with primers PS240/PS241 and using *Xho*I and *Bam*HI to generate *pMIR164b::3XVENUS-N7*. *pMIR164c::3XVENUS-N7* was made by cutting *pMIR164c::GUS* (Baker et al., 2005) with *Xho*I and *Bam*HI and ligating into the pPD35 vector. The *Not*I cassette from each pPD35 subclone was shuttled into the pMLBART (Eshed et al., 1999) binary vector as previously described (Baker et al., 2005).

All plasmid constructs were sequenced in order to detect potential PCR-introduced point mutations and subsequently transformed into plants by *Agrobacterium*-mediated floral dip infiltration (Clough and Bent, 1998).

Microscopy

Protocols for light microscopy (LM) and SEM were as previously described (Baker et al., 2005). Confocal laser scanning microscopy (CLSM) imaging of live plants was performed using a ZEISS LSM 510 Meta using either a 63× 0.95 W or a 40× 0.05 W Achroplan water objective as described (Heisler et al., 2005; Reddy et al., 2004). FM4-64 dye (Molecular Probes) was used as a plasma membrane marker. Specimens of the VENUS-N7/FM4-64 combination were excited with an argon laser that was attenuated to 10% at 514 nm. Single tracking line-scan mode was used in combination with a NFT 635 VIS main dichroic short-pass filter. Each scan represents the mean of two scans. The emission was split by a 545 nm secondary dichroic filter and sent through a 530-600 nm band pass for detection of VENUS, and a 650 nm long-pass filter for FM4-64 signal, respectively. A single tracking line-scan was used for GFP/FM4-64 co-visualization. GFP/FM4-64 specimens were excited using the 488 nm laser line together with a NFT 635 VIS main dichroic short-pass filter in combination with a 545 nm secondary dichroic to split the emission. GFP and FM4-64 were detected using a 505-530 nm band pass and a 650 nm long-pass filter, respectively.

Genotyping

Presence of the *mir164a-4* T-DNA insertion was confirmed by PCR amplification across the junction between the left border of the T-DNA and the genomic DNA by using the primer pair PS321/PS322 (Table 1). The PCR product was sequenced with primer PS323 to confirm the presence of the insertion site. Insertion of the dSpm transposon in the *mir164c-2* allele was confirmed by PCR with primers PS385/PS386/PS387 (Table 1). The resulting ~650 bp PCR fragment was sequenced with primers PS385 and PS386. Genotyping of the *eep1* allele and the *miR164b-1* allele have been described previously (Baker et al., 2005).

Table 1. Primers used in this study

Name	Sequence
PS240	5′-CCGCTCGAGGAACGGTTAACGTGTATTGTAC-3′
PS241	5′-CGCGGATCCTCTTGCTCATCACACACCTTC-3′
PS272	5′-CCCATTTGGACGTGAATGTAGACAC-3′
PS273	5′-GGAATTCCATATGCGTCACCTTCTTCCACTTATGG-3′
PS321	5′-AGAGTTTGTGAAATTTAGGGCAGA-3′
PS322	5′-CCCATTTGGACGTGAATGTAGACAC-3′
PS323	5′-ATATTGACCATCATACTCATTGC-3′
PS385	5′-TACGAATAAGAGCGTCCATTTTAGAGTGA-3′
PS386	5′-TTATTTCATTAACTGCAAGGTCTAGC-3′
PS387	5′-TATCACATGACTTTATTATACTCGTATGC-3′
PS388	5′-TGGAGAAGCAGGGCACGTGC-3′
PS389	5′-TGGAGAAGCAGGGCACGTGCTGGAGAAGCA-3′
PS396	5′-AGACTCCTTCACCGGTTCGT-3′
PS397	5′-AAACCGTCTTTGGACTCGTG-3′

Gene expression analysis

RNA blot analysis was performed essentially as described (Chen, 2004; Reinhart et al., 2002; Williams et al., 2005) with the following modifications. RNA (15 μg) enriched for small RNAs was isolated from *Arabidopsis* plants using the *mir*Vana RNA Isolation Kit (Ambion, cat. #1560) in combination with Plant RNA Isolation Aid (Ambion, cat. #9690) according to the manufacturer's instructions. Blots were hybridized using a [γ-^{32}P]-ATP end-labeled locked nucleic acid ath-*MIR164a* oligonucleotide (Exiqon A/S, Denmark, cat. #30024). A mixture of 0.1 μM PS388/PS389 oligonucleotides were used as 20- and 30-nt size standards, respectively. As a loading control, blots were stripped and re-probed with a [γ-^{32}P]-ATP end-labeled DNA oligonucleotide (5′-TTGCGTGTCATC-CTTGCGCAGG-3′) complementary to U6 RNA (Mallory et al., 2004). ImageJ 1.34s software (http://rsb.info.nih.gov/ij) was used for quantification of *miR164*. Quantitative reverse transcriptase-mediated polymerase chain reaction (qRT-PCR) analyses were performed as described (Baker et al., 2005). Transcript levels were normalized to the level of the non-target gene *TUB4* (*At5g44340*). The primer pairs used to detect transcripts of *TUB4*, *CUC1*, *CUC2*, *NAC1*, *At5g07560* and *At5g61430* were described previously (Mallory et al., 2004). Primer pair PS396/PS397 (Table 1) was used to detect *At5g39610*.

RNA in situ hybridization analyses for *CUC1* and *CUC2* were performed as described (Baker et al., 2005). For the miRNA in situ hybridizations, we followed the protocol of Valoczi and co-workers as originally described (Valoczi et al., 2006). The locked nucleic acid (LNA) miRNA oligos were end-labelled using the DIG Oligonucleotide 3′-End Labelling Kit, 2nd Generation, from Roche (cat. #03 353 575 910) according to the manufacturer's recommendations. LNA-ath-*miR164a* antisense oligo (5′-TGCACGTGCCCTGCTTCTCCA-3′) was used to detect *miR164* miRNAs. Scramble-miR (Exiqon A/S, Denmark, cat. #99001; 5′-TTCACA-ATGCGTTATCGGATGT-3′) was used as a negative control (rather than *miR164* sense probes, which could hybridize to *miR164* target transcripts). Hybridization was performed at 50°C overnight for all slides. A total of five washes were performed at 50°C with 2× SSC-50% formamide. An RNaseA digest was included after the third wash to remove non-specific background signal. Standard blocking and washing steps in combination with anti-DIG antibody (Roche) were used for the immunological detection (Long and Barton, 1998). Western Blue Reagent (Promega) in combination with levamisole was used for the detection reaction. Slides were mounted in Glycerol in TE.

RESULTS

Analysis of *mir164abc* triple-mutant plants reveals functional redundancy among *MIR164* miRNAs

To assess the potential for functional redundancy among the three members of the *MIR164* family of miRNAs, we constructed triple-mutant plants carrying loss-of-function mutations in *MIR164a*, *MIR164b*, and *MIR164c*. A mutant allele for *MIR164a* was isolated from the GABI-Kat collection of transferred DNA (T-DNA) insertion lines (Rosso et al., 2003). This allele was named *mir164a-4*, as three other *mir164a* alleles had been described previously (Guo et al., 2005). *mir164a-4* is likely to represent a null allele because the T-DNA is inserted 29 bp 3′ of the last nucleotide of the processed *miR164a* sequence and thus disrupts the predicted stem-loop structure of the *miR164a* precursor, which is essential for miRNA biogenesis (see Fig. S1 in the supplementary material) (Nikovics et al., 2006; Parizotto et al., 2004). Plants homozygous for *mir164a-4* have been reported to show deepened serration of the leaf margins (see Fig. S2 in the supplementary material) (Nikovics et al., 2006). Shoots of the previously described *mir164b-1* mutant also displayed an essentially normal phenotype (Mallory et al., 2004), whereas *mir164c-1* mutant plants formed extra petals in early-arising flowers, but otherwise largely resembled wild-type plants (Baker et al., 2005). We used these single-mutant lines to generate plants homozygous for *mir164a-4*, *mir164b-1* and *mir164c-1* (henceforth referred to as *mir164abc* triple mutants). The results of RNA blot analyses revealed that in *mir164abc* triple mutants, *miR164*-type 21 nt miRNAs are severely reduced in abundance, if not completely abolished, compared with wild-type plants (Fig. 1A). *mir164abc* triple mutants were indistinguishable from wild-type plants during vegetative development, except for rosette leaves that appeared slightly more serrated in the triple mutant (see Fig. S2 in the supplementary material) (Nikovics et al., 2006). Severe phenotypic alterations were observed, however, after the switch from vegetative to reproductive development. *Arabidopsis* wild-type flowers are composed of an almost invariant number of floral organs, with four sepals, four petals, six stamens, and two fused carpels arranged in four concentric circles or whorls (Fig. 1B). By contrast, most flowers of the *mir164abc* triple mutant had an increased number of sepals and petals, but slightly fewer stamens than L*er* wild-type and *mir164aAbBcC* (L*er*/Col) control plants (Fig. 1C-G, and data not shown). Organ numbers in *mir164abc* triple mutants were highly variable, which is reflected in relatively large standard deviations of the organ counts for flowers at different positions along the stem (Fig. 1F,G). In addition to the organ-number defects, individual organs varied in size and carpels typically failed to fuse in the triple mutants, resulting in a severe reduction in fertility (Fig. 1C-E).

Thus, loss of *miR164a* and *miR164b* function substantially enhances the floral defects of *mir164c* plants, as floral organs are affected in all four whorls and in all flowers independent of their time of initiation (Fig. 1E-G). These miRNAs might therefore control flower development in a redundant manner.

Control of phyllotaxis by *miR164* miRNAs

In addition to the flower defects described above, the phyllotaxis of *mir164abc* triple-mutant plants was severely disrupted (Fig. 2, and see Fig. S3 in the supplementary material). In wild-type plants, flower primordia are successively initiated on the flanks of the inflorescence meristem, so that an incipient primordium is initiated in a position that is furthest away from the two preceding primordia (Reinhardt, 2005). This leads to a spiral arrangement, in which developing flowers are positioned both radially and vertically at regular intervals along the stem (Fig. 2E). By contrast, *mir164abc* triple-mutant plants displayed a highly unequal and distorted arrangement of flowers, both with respect to the angle formed by two consecutive flowers and their distance from each other along the axis of the stem (Fig. 2C,D). The average internode distance (the distance between two flowers) of the mixed L*er*/Col-0 wild-type control was 8.7±3.6 mm (s.d., n_{tot}=149), and 8.6±8.6 mm (s.d., n_{tot}=150) for *mir164abc* triple-mutant plants (Fig. 2K). Thus, the mean internode length was almost unaffected in the *mir164abc* mutant. However, whereas in the wild-type control 87% (129/149) of all flowers remained within the standard deviation of the mean value for the internode distance of the wild type (categories 5 mm to 12 mm), this was true for only 32% (48/150) of *mir164abc* triple-mutant flowers. Notably, in *mir164abc* mutants, 35% of all flowers were separated by a distance of 1 mm or less, compared with fewer than 2% (2/149) in the control (Fig. 2J,K).

The initial positioning of flower primordia, however, was normal in *mir164abc* triple mutants when compared with the wild type (Fig. 2A,B), indicating that the disruption of the phyllotaxis in *miR164abc* mutants occurs after flowers have been initiated. Thus, the positioning of flowers in *Arabidopsis* appears to be dependent not only on their initiation pattern at the shoot apex, but also on mechanisms that actively retain their initial arrangement during flower maturation and growth.

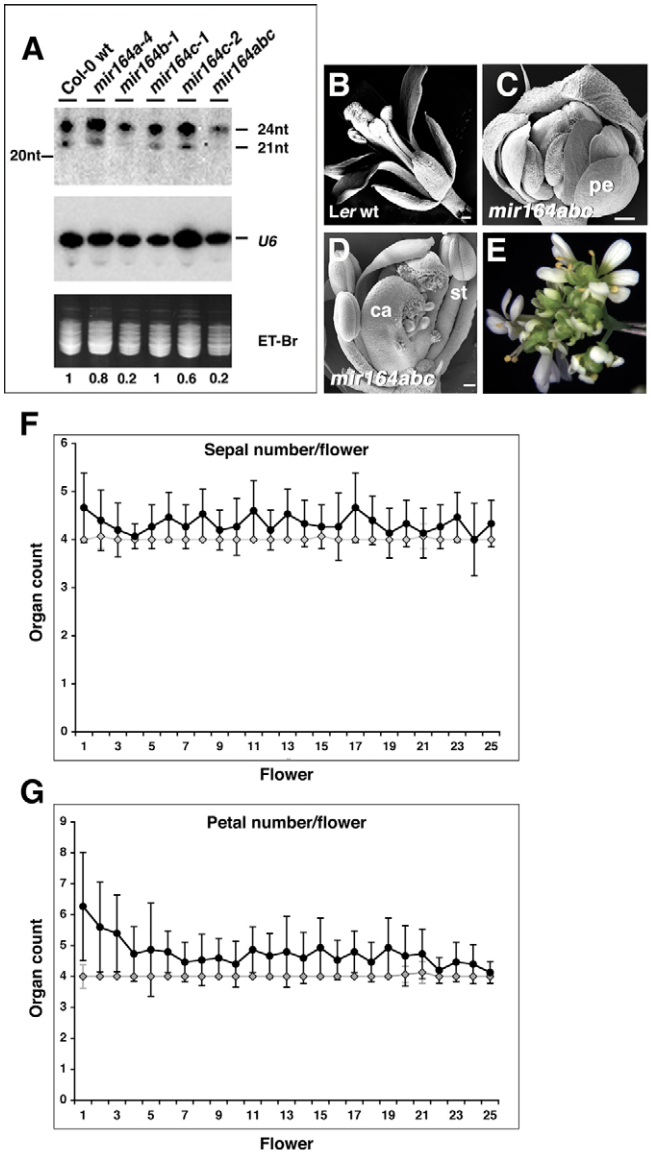

Fig. 1. Floral phenotype of mutant plants impaired in *miR164* biogenesis. (**A**) Quantification of *miR164* abundance in *mir164* mutants. RNA blot analysis of the small RNA fraction isolated from wild-type Col-0, *mir164a-4*, *mir164b-1*, *mir164c-1*, *mir164c-2*, and *mir164a-4 b-1 c-1* triple-mutant inflorescences hybridized with probes complementary to *miR164a* (upper blot) and *U6* small RNA (middle blot), respectively. The ethidium bromide-stained agarose gel is shown beneath (numbers indicate fold-change of *miR164* accumulation with respect to Col-0 wt, which was set to 1). As *miR164a* and *miR164b* differ from *miR164c* in a single nucleotide, different *miR164* miRNAs cannot be distinguished on an RNA blot; thus, signals are derived from all three *miR164* miRNAs. The experiment was repeated twice with the same result. The antisense *MIR164* oligonucleotide probe hybridizes to two distinct RNA size classes, of 21 and ~24 nt, in agreement with previous reports (Dunoyer et al., 2004; Valoczi et al., 2006). It has been proposed that the 21 nt form of *miR164* is the functional entity sufficient to guide target cleavage, for which the ~24 nt form, which has distinct requirements for its biogenesis, appears to be dispensable (Dunoyer et al., 2004). (**B-D**) Results of SEM analysis. (B) Mature (stage 13) wild-type flower of accession L*er*. Flower stages were defined according to Smyth et al. (Smyth et al., 1990). (C) Stage 12 and (D) stage 13 flowers of *mir164abc* triple-mutant plants show variable organ numbers and unfused carpels. Sepals have been removed for better visibility of the inner organs. Scale bars: 200 μm in B; 100 μm in C,D. Abbreviations: pe, petals; ca, carpels; st, stamens. (**E**) A *mir164abc* triple-mutant inflorescence. (**F**,**G**) Charts representing organ counts from *mir164abc* triple-mutant (black) and *mir164aAbBcC* plants (gray), which served as the wild-type control to assess the potential influence of the mixed L*er*/Col-0 background on the phenotypic changes. The average floral organ number ('Organ count') is plotted against each flower position along the stem ('Flower'). Numbers indicate the position of the flower along the stem from the oldest (1) to the youngest (25). Error bars represent s.d. in (F) sepal and (G) petal number. Stamen number was reduced with respect to Col-0 and slightly reduced with respect to the wild-type control. Notably, variability in stamen number, but not in sepal and petal number, increased in the mixed L*er*/Col-0 background, when compared with the Col-0 background (data not shown). Carpel number is only weakly affected in *mir164abc* mutants.

In order to identify the cause of the phyllotaxis defects in *mir164abc* mutants, stem segments were examined by scanning electron microscopy at a position basal to the meristem, where flowers are at an advanced stage of development. Whereas mature flowers were separated by uniformly elongated and rectangular epidermal cells in the wild type (Fig. 2F,H), cells between the clustered flowers of *mir164abc* triple-mutant plants appeared smaller and more variable in shape (Fig. 2G,I). In addition, successive *mir164abc* flowers were often radially separated by only five or six cells (Fig. 2I), which is similar to the number of cells found between two neighboring floral primordia at the time of initiation (Heisler et al., 2005; Reddy et al., 2004). This suggests that in *mir164abc* plants, cell division activities are repressed in the internodes that separate individual flowers.

MIR164 precursors are expressed in partially overlapping domains

In order to determine how the *miR164abc* mutant phenotype correlates with *MIR164* expression, we analyzed the expression patterns for all three members of the *MIR164* family. To enable the detection of expression patterns of individual family members, we used green fluorescent protein (GFP)-based transcriptional reporters. For the construction of the reporters we used the 5′ regulatory regions upstream of the individual miRNA precursor sequences that had been previously reported to be sufficient for compensating for a loss of the individual *miR164* miRNAs (Baker et al., 2005; Guo et al., 2005; Nikovics et al., 2006). Confocal laser scanning microscopy (CLSM) was used to image reporter gene expression in vivo (Fig. 3A-D).

During reproductive development, when phenotypic alterations become apparent in *miR164abc* plants, all three reporter genes were expressed in inflorescence tissue and predominantly in epidermal cells (Fig. 3, and data not shown). For *MIR164c*, GFP fluorescence was detected in the inflorescence meristem, in lateral boundary cells between flower primordia and the inflorescence meristem, as well as in floral meristems, sepal margins and carpels (Fig. 3C,D). Expression of the GFP-based reporter is in agreement with that of the previously described β-glucuronidase-based transcriptional reporter for *MIR164c* (Baker et al., 2005), which showed expression in meristems and young floral buds. *MIR164a* reporter expression

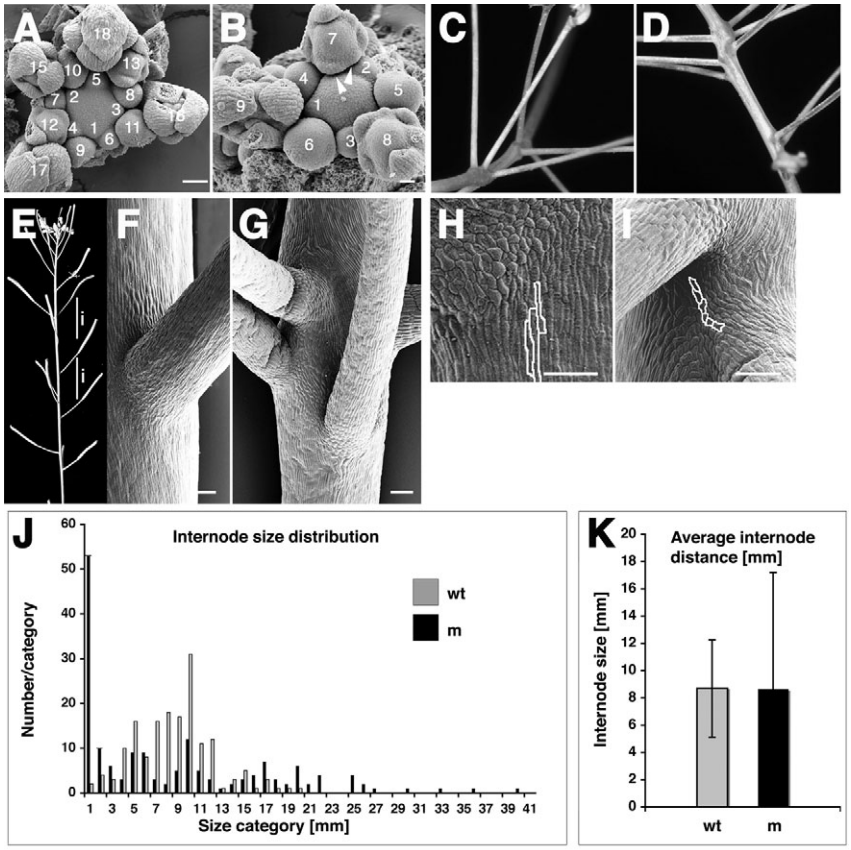

Fig. 2. Phyllotaxis defects of *mir164abc* triple-mutant plants. (**A**,**B**,**F-I**) SEM pictures and (**C-E**) photographs of Col-0 wild-type plants (A,E,F,H) and *mir164abc* mutants (B,C,D,G,I). (A,B) Initiating flower primordia follow a spiral phyllotactic pattern in the wild type (A) and in *mir164abc* triple mutants (B). Numbers indicate the succession of floral bud initiation. (B) Arrowheads in B point to sepal primordia of different sizes. (C-E) Flowers of *mir164abc* triple-mutant plants are arranged randomly along the stem (C,D) when compared with the regular pattern of Col-0 wild-type flowers (E). i, internode. (F-I) Stem internodes are uniformly covered with long and rectangular epidermal cells in the wild type (F,H), whereas clustered flowers in *mir164abc* triple-mutant plants are separated by few, variably shaped non-elongate cells (G,I). In H,I, the margins of equivalent cells are highlighted to demonstrate the differences in cell shape and size. (**J**) Distribution of size classes, each comprising a specific internode length. The number of internodes ('Number/category') falling into a specific size category are plotted against the size categories ('Size category [mm]'). The internode sizes of the mixed L*er*/Col-0 wild-type control (wt, gray) are distributed around the mean value 8.7±3.6 (s.d., n_{tot}=149), whereas internode distribution of the *mir164abc* mutant (m, black) does not follow a similar pattern. (**K**) The average internode distance (in mm) is 8.7±3.6 (s.d., n_{tot}=149) for the wild-type control (wt, gray) and 8.6±8.6 (s.d., n_{tot}=150) for *mir164abc* triple-mutant (m, black) plants. Error bars indicate s.d. Scale bars: 20 μm in A,B; 100 μm in F-I.

was detected in leaves (Nikovics et al., 2006), and it was observed in the boundaries between the inflorescence meristem and floral primordia, in young floral buds [stages 2-4; stages according to Smyth et al. (Smyth et al., 1990)], as well as in the adaxial domains of older flowers (Fig. 3A). Thus, the expression patterns of *MIR164a* and *MIR164c* are partially overlapping and are consistent with the regions of the plant affected in *mir164abc* triple-mutants. By contrast, GFP expression in the *MIR164b* reporter line appeared to be excluded from meristems and was strongest in abaxial epidermal cells of sepals (Fig. 3B). The RNA blot analysis (Fig. 1A) suggests that the *miR164b* locus contributes substantially to the overall population of *miR164* RNA molecules in the inflorescence. However, it is unknown whether the three *miR164* miRNAs are equally well processed, or how the efficiency of processing varies among cells, which may explain the apparent discrepancy between the results obtained in the RNA blot analysis and those obtained through the use of the transcriptional reporter. Alternatively, additional regulatory sequences that could affect the degree of *miR164b* accumulation may not have been included in the reporter construct.

In addition to expression during the reproductive phase of development, we also detected GFP expression in the *MIR164a* and the *MIR164c* reporter lines in certain vegetative tissues (see Fig. S4 in the supplementary material). In summary, the results of our expression analyses suggest that the different members of the *MIR164* family are expressed in distinct patterns during plant development, and that their expression patterns overlap only partially.

Mature *miR164* miRNAs are essentially identical in sequence and are predicted to target the same set of transcripts. However, the availability of the triple *mir164abc* mutant, as well as of the various double mutants, allowed the use of in situ hybridization to infer characteristics of the expression patterns of the individual *MIR164* family members. DIG-labeled LNA oligo probes were used to detect *miR164* miRNA accumulation patterns on tissue sections of inflorescences. In L*er* wild-type plants, combined signal of all three *miR164* miRNAs was detected in vegetative leaves, in inflorescence meristems, in young flower primordia as well as in floral organ primordia. Strong signal was also detected in the locules of the anthers (Fig. 3E,F). The *miR164* expression pattern in *A. thaliana* thus resembled the pattern of *miR164* expression in *N. benthamiana* (Valoczi et al., 2006). There was no signal above background in the Scramble-miR control (Fig. 3G,H), and thus the detected signal was *miR164*-specific. Weak, but specific signal was also detected in the *mir164abc* triple-mutant background (Fig. 3O,P). This signal might represent processed *miR164* originating from leaky expression of one or more of the three *mir164* mutant loci. Alternatively, the probe might hybridize to another RNA fragment, for instance to the ~24 nt band that was detected on the RNA blot (Fig. 1A). *miR164c* accumulation, as detected in *mir164a-4 b-1* double-mutant plants (Fig. 3I,J), was found in the expected tissue but did not accumulate to levels significantly above the level of *miR164* signal observed in *mir164abc* triple mutants. *miR164b* on the other hand, as detected in *mir164a-4 c-1* double mutants, reached a level of expression that was comparable to *miR164* accumulation in the wild type (Fig. 3K,L). Accumulation of *miR164a*, when examined in *mir164b-1 c-1* double-mutant plants was comparable to the result obtained for *miR164c*, with the difference that the expression in leaves remained strong in *mir164b-1 c-1* double mutants (Fig. 3M,N).

Altogether, the in situ hybridization data are consistent with the results obtained from RNA blot experiments, which indicate that *miR164b* miRNAs contribute substantially to the *miR164* miRNA pool in shoots.

miR164 miRNAs regulate the abundance of all predicted target transcripts

The *miR164* miRNAs were all predicted previously to target six members of the transcription factor-encoding NAC family, including *CUC1*, *CUC2* and *NAC1* (Rhoades et al., 2002). Cleavage products of the target transcripts that are consistent with *miR164* miRNA-dependent degradation were detected in wild-type plants (Guo et al., 2005; Kasschau et al., 2003; Mallory et al., 2004). Analysis of *mir164* single mutants showed that *CUC1* and *CUC2* transcript levels, but not those of the other predicted targets, are elevated in shoot apices of *mir164c* plants as compared with the wild type (Baker et al., 2005), and that *NAC1* transcripts are enriched in roots of *mir164a* and *mir164b* mutants (Guo et al., 2005). Furthermore, expression of *miR164* from the constitutive 35S promoter led to a reduction in transcript levels of the predicted targets (Guo et al., 2005; Laufs et al., 2004), indicating that these transcripts can be under miRNA-dependent regulation when *miR164* miRNAs are ectopically expressed. However, the individual *miR164* miRNAs are not expressed ubiquitously, but rather in specific patterns (Fig. 3). Thus, it is possible that certain targets, at least in some tissues, are not regulated by miRNAs because their expression domains and those of the *MIR164* genes do not overlap.

To test whether all of the predicted targets are subjected to miRNA-dependent regulation and whether there are tissue-specific differences in the degree to which individual transcripts are controlled by *miR164* miRNAs, their transcript levels were measured in inflorescences, rosette leaves and seedlings of *mir164abc* triple-mutant plants by qRT-PCR. All of the predicted targets accumulated in *mir164abc* mutants to higher levels than in wild-type plants (Fig. 4A-C), confirming that they are indeed regulated by the endogenous *miR164* miRNAs. Moreover, the extent to which transcripts of the targets accumulated in the different tissue samples varied substantially, indicating tissue-specific effects of *miR164* miRNAs on target gene expression. These differences might be due to variable degrees of overlap between regions of target gene and miRNA expression in the tissues tested.

Regulation of *CUC* gene expression by *miR164* miRNAs

It has been proposed that miRNAs control development by selectively clearing cells of mRNAs that encode cell fate determinants, thereby promoting rapid cell fate transitions and differentiation of cell lineages (Rhoades et al., 2002). In accordance with this idea, the plant miRNAs *miR171*, *miR172* and *miR165/166* and their respective target mRNAs were found in adjacent, but non-overlapping domains (Chen, 2004; Juarez et al., 2004; Kidner and Martienssen, 2004; Parizotto et al., 2004; Williams et al., 2005). For *miR164* miRNAs, however, a different mechanism for the control of target gene expression has been proposed. In *mir164c* single mutants, transcripts of *CUC1* and *CUC2* were found to be elevated when compared with the wild type, but remained restricted to cells in boundary regions (Baker et al., 2005), implying that *miR164c* does not act by clearing *CUC1* and *CUC2* mRNAs from non-boundary cells, but rather by regulating transcript abundance in a pre-existing pattern.

In addition to *miR164c*, *miR164a* and *miR164b* are also likely to be involved in regulating *CUC1* and *CUC2* expression, as inactivation of *miR164a* and *miR164b* leads to an enhancement of

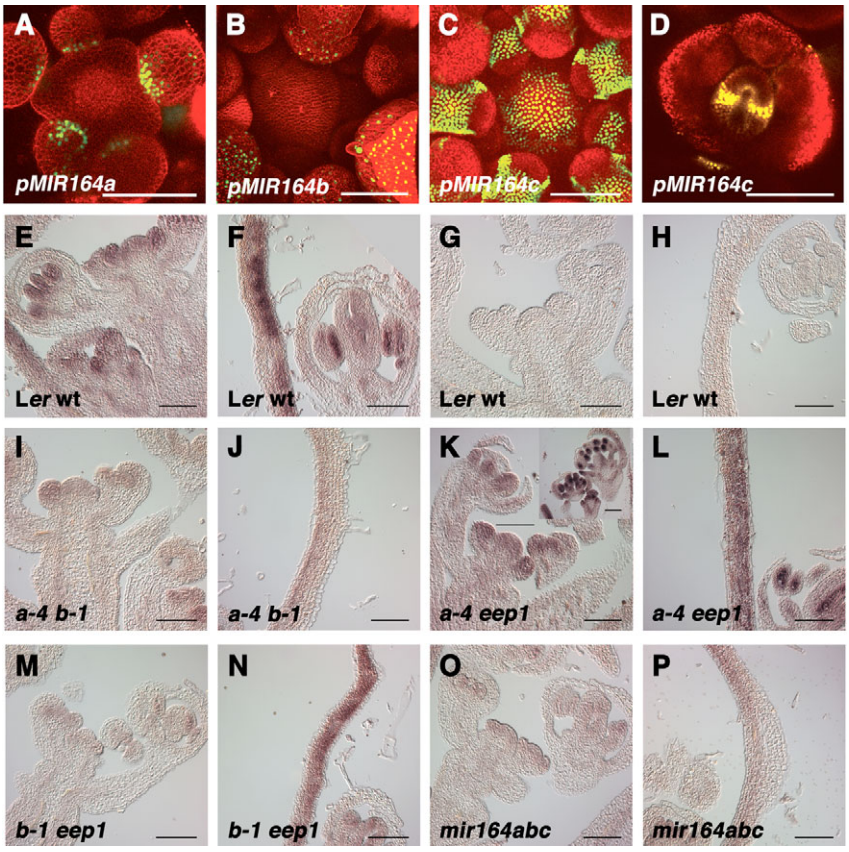

Fig. 3. Expression patterns of *miR164* miRNAs in wild-type plants. (**A-D**) Confocal images of inflorescences. Each transgenic plant expresses the GFP variant 3xVENUS-N7 (green/yellow) under control of the individual miRNA regulatory sequences (as indicated). In A,B, FM4-64 dye was used to stain plasma membranes (red); in C,D, organ outlines are highlighted by red chlorophyll autofluorescence. T1 plants were examined and representative expression patterns are shown. The number of plants showing depicted expression pattern (x) with respect to total sample size (n_{tot}), indicated as ratio (x/n_{tot}), was 7/7 (A), 2*/20 (B) and 5/5 (C,D). *No expression was detected in 18 out of 20 transgenic lines harboring *pMIR164b::3xVENUS-N7*. (**E-P**) In situ hybridization analysis of *miR164* miRNA distribution (E,F,I-P) using DIG-labeled LNA-ath-*miR164a* antisense oligos, in L*er* wild-type (E,F), in *mir164a-4 b-1* double-mutant (I,J), in *mir164a-4 c-1* double-mutant (K,L), in *mir164b-1 c-1* double-mutant (M,N) and in *mir164abc* triple-mutant (O,P) plants. The inset in K shows *mir164* accumulation in developing flowers. (G,H) No signal above background was detected when DIG-labeled Scramble-miR LNA-oligo was used as a control probe on L*er* wild-type tissue. Scale bars: 100 μm.

the defects shown by *mir164c* plants (Figs 1 and 2). The possibility of additional effects of *miR164*-dependent regulation on *CUC1* and *CUC2* expression was tested by examination of the distribution of wild-type *CUC1* and *CUC2* and of miRNA cleavage-resistant versions of these genes (*CUC1*^{m} and *CUC2*^{m}), translationally fused to GFP and expressed from their own promoters, in wild-type plants. CUC1-GFP and CUC2-GFP fusion proteins were detected by CSLM in narrow columns of cells that separate flower primordia and the inflorescence meristem (Fig. 5A,B), in agreement with the reported boundary-specific expression of the corresponding genes (Aida et al., 1999; Takada et al., 2001). By contrast, the miRNA-resistant versions CUC1^{m}-GFP and CUC2^{m}-GFP accumulated in boundaries to much higher levels than the wild-type proteins, as well as weakly in the center of meristems (Fig. 5, compare C,D with A,B, respectively). These differences in protein accumulation strongly suggest that *miR164* miRNAs function by dampening the transcript levels of *CUC1* and *CUC2*, so that the initially strong expression in boundary regions is greatly reduced, whereas the weak expression in meristems is repressed below the detection limit of CLSM. These results also imply that miRNA-dependent regulation is not required per se for the expression of *CUC1* and *CUC2* in boundaries, and thus that the establishment of the expression patterns for these genes is largely under transcriptional control. In agreement with this idea, transcriptional reporters for *CUC1* and *CUC2* showed strong expression in the expected pattern (Fig. 5E,F).

To further investigate the role of *miR164* miRNAs in controlling target transcript abundance, expression of *CUC1* and *CUC2* was examined by in situ hybridization in tissues that are affected in

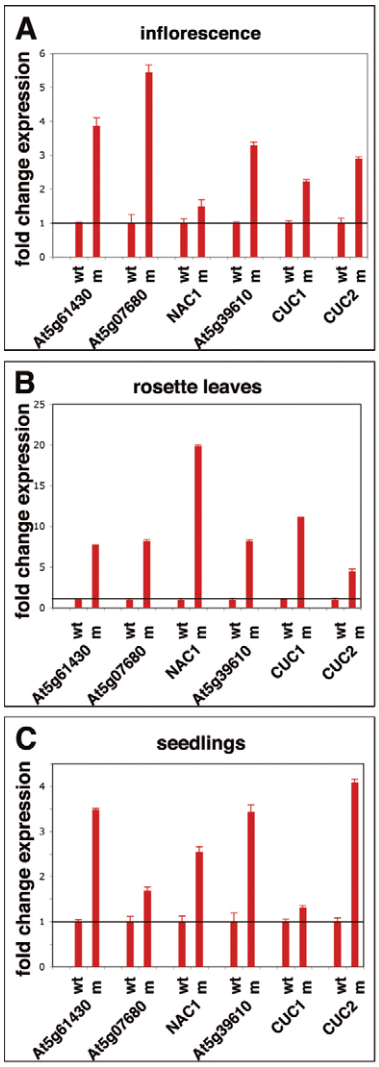

Fig. 4. Loss of *miR164* miRNA-mediated regulation quantitatively affects target gene expression. (**A-C**) Bar charts showing the results of relative qRT-PCR experiments, in which the target transcript abundance was assessed for different tissue types (as indicated) of wild-type and *mir164abc* triple-mutant plants. Results were normalized using *TUB4* transcript levels. The transcript abundance of all predicted *miR164* targets is higher in the *mir164abc* triple mutant (m) as compared with the wild type (wt) in all tissues tested. Fold-change differences in transcript levels between the wild type and the *mir164abc* triple mutant are shown. Bars represent the s.e. of the measurements.

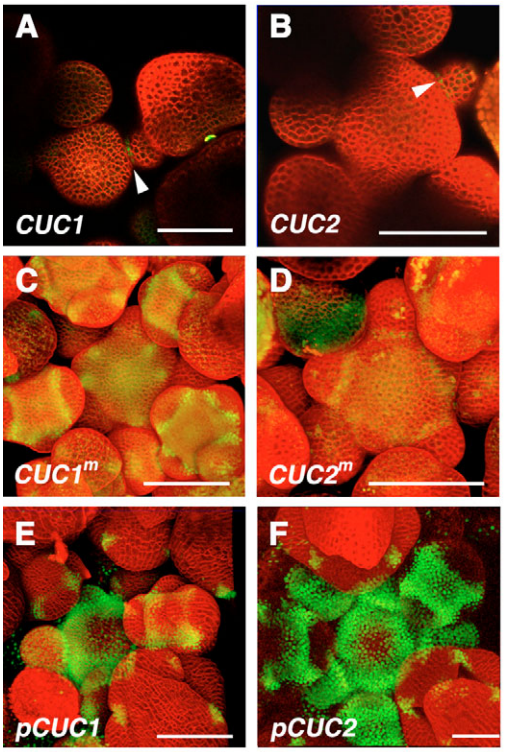

Fig. 5. Effect of *miR164* miRNA regulation on target gene expression. Representative confocal images of inflorescences of primary transformants. FM4-64 dye was used to stain plasma membranes (red). (**A-D**) Effects of *miR164*-mediated regulation on *CUC1* and *CUC2* expression. Consequences of permitted (A,B) and abolished (C,D) *miR164*-mediated regulation for translational fusions of CUC1 (A,C) and CUC2 (B,D) to GFP. The same confocal microscopy settings have been used for the images shown. Arrowheads (A,B) mark cells that weakly express GFP in boundaries between the inflorescence meristem and flower primordia. (**E**,**F**) Transcriptional reporters for *CUC1* (E) and *CUC2* (F) expressing the GFP variant 3xVENUS-N7 (green). Number of plants showing depicted expression pattern (x) with respect to total sample size (n_{tot}), indicated as ratio (x/n_{tot}), was 7/9 for *pCUC1::CUC1-GFP* (A), 6/6 for *pCUC1::CUC1*^{m}*-GFP* (C), 10*/20 (*no expression detected in others) for *pCUC2::CUC2-GFP* (B), 4/4 for *pCUC2::CUC2*^{m}*-GFP* (D), 7/8 for *pCUC1::3xVENUS-N7* (E) and 6/7 for *pCUC2::3xVENUS-N7* (F). Scale bars: 100 μm.

mir164abc triple-mutant plants. Analysis of transverse sections of flowers revealed that *CUC2* expression is strongly upregulated in carpel margin tissue in *mir164abc* plants (Fig. 6B, arrow), as compared with the wild type (Fig. 6A), whereas expression levels in stamens appeared to be unaffected. These tissue-specific differences in *CUC2* transcript accumulation correlate with the expression pattern of *MIR164c*, which is strongly expressed in carpel margin tissue but not detected in stamen primordia (Fig. 3D). These results, together with the observation that the carpel fusion defects of *mir164c* and *mir164abc* plants were not observed in *CUC1*^{m}-expressing plants (Baker et al., 2005) (this study), suggest that overexpression of *CUC2*, and not of *CUC1*, is responsible for this aspect of the mutant phenotype. For *CUC1*, elevated levels of transcript accumulation were seen in inflorescences of *mir164abc* triple-mutant plants within the normal domain of expression (Fig. 6D,F) as compared with wild type (Fig. 6C,E). In addition, expression was observed in apparently random patches of cells within and especially in between floral primordia (Fig. 6D,F), where cell division activities are often reduced in the triple mutant (Fig. 2). Thus, certain phenotypic alterations of *mir164abc* plants, such as the carpel fusion defect and the reduced growth between flower primordia, are tightly correlated with ectopic target transcript accumulation.

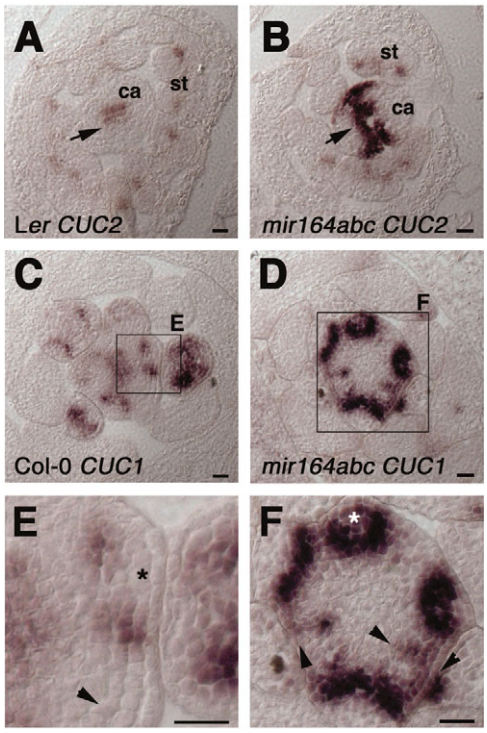

Fig. 6. Target mRNA accumulation in *mir164abc* triple mutants. (**A-F**) In situ localization of *CUC2* (A,B) and *CUC1* (C-F) transcripts in transverse sections of stage 9 flowers (A,B) and of inflorescences (C-F). Tissue of wild-type (A,C,E) and *mir164abc* mutant (B,D,F) plants was processed equivalently and was present on the same microscope slide (A,B), or was hybridized in the same slide sandwich (C,D), to allow a direct comparison of the signals obtained. Arrows (A,B) point to regions of elevated *CUC2* expression in partially fused carpels (ca) of *mir164abc* mutants as compared with the wild type. By contrast, *CUC2* expression in stamens (st) appeared to be unaffected. (C,D and their enlargements E,F) Randomly located foci of high *CUC1* expression were sometimes observed within primordia (asterisks) and between primordia (arrowheads) of *mir164abc* mutant plants. Scale bars: 20 μm.

CUC1 and CUC2 function as growth inhibitors

The ectopic expression of *CUC1* in regions that show reduced cell proliferation in the *miR164abc* triple mutant (Fig. 6) raised the possibility that CUC transcription factors may function by inhibiting cell division activities. To test this, we re-examined transgenic plants expressing *miR164* cleavage-resistant versions of *CUC1* and *CUC2* under the control of the strong, constitutive 35S promoter (Baker et al., 2005). These plants form flowers with misshapen sepals, petals and stamens, which are significantly reduced in size compared with the organs of wild-type flowers (Baker et al., 2005). To determine whether these growth defects are a consequence of reduced cell division rates, a decrease in cell elongation, or both, we examined the abaxial epidermis of sepals of *35S::CUC1*^{m}*-GFP* plants (Fig. 7C), which were about fourfold shorter than those of the wild type (Fig. 7E). Compared with wild-type sepals (Fig. 7A) and those of *miR164abc* triple mutants (Fig. 7B), the average size of the epidermal cells was not significantly changed in the *CUC1*-overexpressor lines (Fig. 7D,F,G). Thus, the dramatically reduced length of sepals of the transgenic plants is not caused by an inhibition of cell elongation, and therefore must be due to a reduction in cell number, suggesting that *CUC* genes function by repressing cell division. The elevated levels of CUC activity in between floral primordia, where growth is severely reduced in *mir164abc* triple-mutant plants, might lead to a suppression of growth between neighboring primordia, thus keeping primordia together while the stem continues to grow. Similarly, the expansion of the *CUC* expression domain in *mir164abc* triple mutants into meristems (Figs 5 and 6) might interfere with primordium formation in the flower and hence cause organ-number defects.

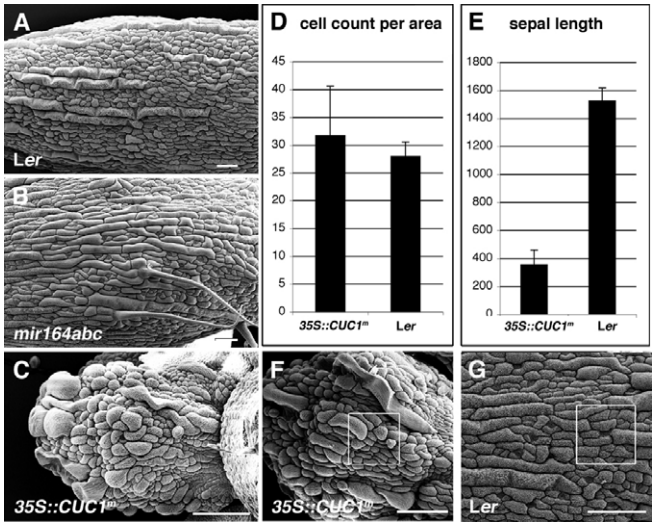

Fig. 7. CUC1 acts as a growth antagonist. (**A-C**) SEM images of the (abaxial) sepal epidermis of wild-type L*er* (A), *mir164abc* triple-mutant (B), and *35S::CUC1*^{m}*-GFP* transgenic plants (C). The sepals of *mir164abc* mutants were typically narrower than, but otherwise indistinguishable from, wild-type sepals (compare B with A). (**D-G**) The bar chart in D depicts the average number of epidermal sepal cells touching a 100 μm by 100 μm square projected onto the central abaxial region of sepals of wild-type (G) and *35S::CUC1*^{m}*-GFP* transgenic plants (F). The average cell number per 0.01mm^2 was 31.8±8.8 (s.d., n_{tot}=10) for *35S::CUC1*^{m}*-GFP* transgenic plants and 28.1±2.5 (s.d., n_{tot}=11) for L*er* wild-type sepals. The bar chart in E depicts the average sepal length of *35S::CUC1*^{m}*-GFP* and wild-type plants. The average sepal length was 360±101 μm (s.d., n_{tot}=10) for *35S::CUC1*^{m}*-GFP* plants and 1529±89 μm (s.d., n_{tot}=9) for L*er* wild-type plants. Scale bars: 100 μm.

DISCUSSION

Functional redundancy and specialization among *miR164* miRNAs

In this study, we have analyzed the potential for functional redundancy among plant miRNAs by studying the effects that inactivation of the entire *MIR164* family has on shoot development. We found that *mir164abc* triple-mutant plants are characterized by severe defects in flower development and phyllotaxis that are not observed in plants in which only individual *MIR164* genes are disrupted. These results indicate that *miR164* miRNAs control shoot development in a redundant manner. However, the degree to which individual *miR164* miRNAs contribute to the regulation of different developmental processes varies. Whereas *mir164a* and *mir164b* single mutants exhibit no obvious defects in shoot development, *mir164c* plants have floral defects that are similar to, but weaker than, those of the *mir164abc* triple mutant. Thus, *mir164c* contributes to a larger extent to the control of flower development than its two sister miRNAs. In the control of phyllotaxis, however, all three miRNAs appear to function in an equal manner, as none of the *mir164* single mutants exhibits any discernable alteration in the arrangement of flowers. Because the *miR164* miRNAs are essentially identical in sequence and have the same target specificities, it is likely that the differences in expression patterns that we have detected in our analysis for the individual family members (Fig. 3), account for their functional diversification.

Functional redundancy is often found in plants, as well as in animals, among protein-coding genes that originated from gene or genome duplications. Although gene duplicates are thought to be often lost over time, retaining duplicated genes can be beneficial for an organism because they might buffer fundamental developmental processes from the detrimental effects of random mutations (Chapman et al., 2006). It is also possible that duplicated genes functionally diverge over time and undergo functional specialization (subfunctionalization), or acquire functions other than that of the progenitor gene (neofunctionalization). These processes are often a result of mutations in the regulatory regions of the gene duplicates that can lead to distinct spatial and/or temporal expression patterns. It has been proposed that miRNAs evolved from their targets by inverted duplication (Allen et al., 2004), and recent evidence suggests that large-scale segmental duplications may play a key role in the establishment of miRNA families in plants, including the *MIR164* family (Maher et al., 2006). Thus, miRNA genes might evolve similarly to protein-coding genes. The finding that the *miR164* miRNAs, though largely functionally redundant, contribute differently to certain aspects of development is therefore in agreement with functional diversification through subfunctionalization, an idea that is further supported by the distinct, but partially overlapping expression patterns of the individual *MIR164* miRNA genes.

miR164 miRNAs contribute to the robustness of development

The absence of *miR164* miRNAs leads to phenotypic alterations that are correlated with elevated and/or ectopic target transcript accumulation. This suggests that the role of *miR164* miRNAs in development is to prevent fluctuations in target gene expression and, thus, to increase the precision of the developmental programs underlying organogenesis and to protect them from the intrinsic stochasticity of biochemical processes such as transcription and translation. *miR164* miRNAs appear to control development by dampening transcript accumulation of their targets, where their expression patterns and those of the targets overlap. Furthermore, *CUC1* and *CUC2* expression domains are enlarged in *mir164abc* mutant inflorescence meristems (Fig. 6), indicating that the *miR164* miRNAs can spatially limit target mRNA accumulation in addition to reducing the levels of target transcripts. These seemingly different effects are likely to be a consequence of spatial differences in target transcript accumulation. Where target gene expression is high, the pool of *miR164* miRNAs might not suffice to efficiently clear the target transcripts from cells. By contrast, the level of *miR164* miRNAs may be high enough to completely eliminate target transcripts where they are expressed at comparatively low levels. This mode of action would be consistent with findings that showed an miRNA-dependent reduction, but not an elimination, of highly expressed transcripts in mammalian tissues (Farh et al., 2005; Sood et al., 2006), as well as with the results of a recent study that reported *miR168* and its target *AGO1* as being co-expressed in *Arabidopsis* (Vaucheret et al., 2006). Thus, dampening of gene expression is a mechanism of miRNA-target interaction that is likely to be found in both plants and animals.

The ability of miRNAs to reduce fluctuations in transcript abundance suggests that miRNAs may be involved in buffering developmental processes. In the absence of the *miR164* miRNAs, the domain of *CUC* expression is less precise and can expand seemingly at random from boundary regions into peripheral regions of the inflorescence meristem and also into flower primordia (Fig. 6). This indicates that transcriptional control per se lacks the accuracy to prevent fluctuations in the *CUC* expression domains. The variability in flower positioning in *mir164abc* mutants correlates with local alterations in the *CUC* expression pattern and can be explained by the lack of precision in the control of the *CUC* expression domain. These observations are in agreement with a role in stabilizing developmental processes, a function that has also been proposed for animal miRNAs (Hornstein and Shomron, 2006).

We thank Drs J. Fletcher, L. Williams and A. Mallory for protocols; Drs J. Long and P. Das for plasmids; A. Garda for technical assistance; and Drs A. Roeder, M. Heisler, C. Ohno and Z. Nimchuk for comments on the manuscript. We are indebted to members of the Meyerowitz laboratory, especially Dr C. Baker, for stimulating discussions, and to Prof. Dr U. Grossniklaus for his support of P.S. This work was supported by National Science Foundation grant MCB-0520193 to J.L.R. and E.M.M., by the Millard and Muriel Jacobs Genetics and Genomics Laboratory at the California Institute of Technology, and by a European Molecular Biology Organization long-term fellowship (ALTF 460-2003) and a Forschungskredit from the University of Zurich to P.S. J.G. was supported by a grant from the Swiss National Science Foundation to Ueli Grossniklaus.

Supplementary material

Supplementary material for this article is available at
http://dev.biologists.org/cgi/content/full/134/6/1051/DC1

References

Abbott, A. L., Alvarez-Saavedra, E., Miska, E. A., Lau, N. C., Bartel, D. P., Horvitz, H. R. and Ambros, V. (2005). The let-7 MicroRNA family members mir-48, mir-84, and mir-241 function together to regulate developmental timing in Caenorhabditis elegans. *Dev. Cell* **9**, 403-414.

Aida, M., Ishida, T., Fukaki, H., Fujisawa, H. and Tasaka, M. (1997). Genes involved in organ separation in Arabidopsis: an analysis of the cup-shaped cotyledon mutant. *Plant Cell* **9**, 841-857.

Aida, M., Ishida, T. and Tasaka, M. (1999). Shoot apical meristem and cotyledon formation during *Arabidopsis* embryogenesis: interaction among the *CUP-SHAPED COTYLEDON* and *SHOOT MERISTEMLESS* genes. *Development* **126**, 1563-1570.

Allen, E., Xie, Z., Gustafson, A. M., Sung, G. H., Spatafora, J. W. and Carrington, J. C. (2004). Evolution of microRNA genes by inverted duplication of target gene sequences in Arabidopsis thaliana. *Nat. Genet.* **36**, 1282-1290.

Aukerman, M. and Sakai, H. (2003). Regulation of flowering time and floral organ identity by a microRNA and its *APETALA2*-like target genes. *Plant Cell* **15**, 2730-2741.

Baker, C. C., Sieber, P., Wellmer, F. and Meyerowitz, E. M. (2005). The *early extra petals1* mutant uncovers a role for microRNA *miR164c* in regulating petal number in Arabidopsis. *Curr. Biol.* **15**, 303-315.

Bartel, D. P. (2004). MicroRNAs: genomics, biogenesis, mechanism, and function. *Cell* **116**, 281-297.
Baulcombe, D. (2004). RNA silencing in plants. *Nature* **431**, 356-363.
Chapman, B. A., Bowers, J. E., Feltus, F. A. and Paterson, A. H. (2006). Buffering of crucial functions by paleologous duplicated genes may contribute cyclicality to angiosperm genome duplication. *Proc. Natl. Acad. Sci. USA* **103**, 2730-2735.
Chen, X. (2005). micro RNA biogenesis and function in plants. *FEBS Lett.* **579**, 5923-5931.
Chen, X. M. (2004). A miRNA as a translational repressor of *APETALA2* in *Arabidopsis* flower development. *Science* **303**, 2022-2025.
Clough, S. J. and Bent, A. F. (1998). Floral dip: a simplified method for Agrobacterium-mediated transformation of Arabidopsis thaliana. *Plant J.* **16**, 735-743.
Dunoyer, P., Lecellier, C. H., Parizotto, E. A., Himber, C. and Voinnet, O. (2004). Probing the microRNA and small interfering RNA pathways with virus-encoded suppressors of RNA silencing. *Plant Cell* **16**, 1235-1250.
Eshed, Y., Baum, S. F. and Bowman, J. L. (1999). Distinct mechanisms promote polarity establishment in carpels of *Arabidopsis*. *Cell* **99**, 199-209.
Farh, K. K., Grimson, A., Jan, C., Lewis, B. P., Johnston, W. K., Lim, L. P., Burge, C. B. and Bartel, D. P. (2005). The widespread impact of mammalian MicroRNAs on mRNA repression and evolution. *Science* **310**, 1817-1821.
Guo, H. S., Xie, Q., Fei, J. F. and Chua, N. H. (2005). MicroRNA directs mRNA cleavage of the transcription factor NAC1 to downregulate auxin signals for arabidopsis lateral root development. *Plant Cell* **17**, 1376-1386.
Heisler, M., Ohno, C., Das, P., Sieber, P., Reddy, G. V. and Meyerowitz, E. M. (2005). Patterns of auxin transport and gene expression during primordium development revealed by live imaging of the Arabidopsis inflorescence mersistem. *Curr. Biol.* **15**, 1899-1911.
Hornstein, E. and Shomron, N. (2006). Canalization of development by microRNAs. *Nat. Genet.* **38**, S20-S24.
Juarez, M., Kui, J., Thomas, J., Heller, B. and Timmermans, M. (2004). microRNA-mediated repression of *rolled leaf1* specifies maize leaf polarity. *Nature* **428**, 84-88.
Kasschau, K. D., Xie, Z. X., Allen, E., Llave, C., Chapman, E. J., Krizan, K. A. and Carrington, J. C. (2003). P1/HC-Pro, a viral suppressor of RNA silencing, interferes with *Arabidopsis* development and miRNA function. *Dev. Cell* **4**, 205-217.
Kidner, C. A. and Martienssen, R. (2004). Spatially restricted microRNA directs leaf polarity through ARGONAUTE1. *Nature* **428**, 81-84.
Kim, J., Jung, J. H., Reyes, J. L., Kim, Y. S., Kim, S. Y., Chung, K. S., Kim, J. A., Lee, M., Lee, Y., Narry Kim, V. et al. (2005). microRNA-directed cleavage of ATHB15 mRNA regulates vascular development in Arabidopsis inflorescence stems. *Plant J.* **42**, 84-94.
Laufs, P., Peaucelle, A., Morin, H. and Traas, J. (2004). MicroRNA regulation of the *CUC* genes is required for boundary size control in *Arabidopsis* meristems. *Development* **131**, 4311-4322.
Lim, L. P., Lau, N. C., Garrett-Engele, P., Grimson, A., Schelter, J. M., Castle, J., Bartel, D. P., Linsley, P. S. and Johnson, J. M. (2005). Microarray analysis shows that some microRNAs downregulate large numbers of target mRNAs. *Nature* **433**, 769-773.
Llave, C., Xie, Z. X., Kasschau, K. D. and Carrington, J. C. (2002). Cleavage of *SCARECROW*-like mRNA targets directed by a class of *Arabidopsis* miRNA. *Science* **297**, 2053-2056.
Long, J. A. and Barton, M. K. (1998). The development of apical embryonic pattern in *Arabidopsis*. *Development* **125**, 3027-3035.
Lu, C., Kulkarni, K., Souret, F. F., MuthuValliappan, R., Tej, S. S., Poethig, R. S., Henderson, I. R., Jacobsen, S. E., Wang, W., Green, P. J. et al. (2006). MicroRNAs and other small RNAs enriched in the Arabidopsis RNA-dependent RNA polymerase-2 mutant. *Genome Res.* **16**, 1276-1288.
Maher, C., Stein, L. and Ware, D. (2006). Evolution of Arabidopsis microRNA families through duplication events. *Genome Res.* **16**, 510-519.
Mallory, A. C. and Vaucheret, H. (2006). Functions of microRNAs and related small RNAs in plants. *Nat. Genet.* **38**, S31-S36.
Mallory, A. C., Dugas, D. V., Bartel, D. P. and Bartel, B. (2004). MicroRNA regulation of NAC-domain targets is required for proper formation and separation of adjacent embryonic, vegetative, and floral organs. *Curr. Biol.* **14**, 1035-1046.
Nikovics, K., Blein, T., Peaucelle, A., Ishida, T., Morin, H., Aida, M. and Laufs, P. (2006). The balance between the *MIR164A* and *CUC2* genes controls leaf margin serration in Arabidopsis. *Plant Cell* **18**, 2929-2945.
Palatnik, J. F., Allen, E., Wu, X. L., Schommer, C., Schwab, R., Carrington, J. C. and Weigel, D. (2003). Control of leaf morphogenesis by microRNAs. *Nature* **425**, 257-263.
Parizotto, E. A., Dunoyer, P., Rahm, N., Himber, C. and Voinnet, O. (2004). In vivo investigation of the transcription, processing, endonucleolytic activity, and functional relevance of the spatial distribution of a plant miRNA. *Genes Dev.* **18**, 2237-2242.
Park, W., Li, J. J., Song, R. T., Messing, J. and Chen, X. M. (2002). CARPEL FACTORY, a Dicer homolog, and HEN1, a novel protein, act in microRNA metabolism in *Arabidopsis thaliana*. *Curr. Biol.* **12**, 1484-1495.
Rajagopalan, R., Vaucheret, H., Trejo, J. and Bartel, D. P. (2006). A diverse and evolutionarily fluid set of microRNAs in Arabidopsis thaliana. *Genes Dev.* **20**, 3407-3425.
Reddy, G. V., Heisler, M. G., Ehrhardt, D. W. and Meyerowitz, E. M. (2004). Real-time lineage analysis reveals oriented cell divisions associated with morphogenesis at the shoot apex of Arabidopsis thaliana. *Development* **131**, 4225-4237.
Reinhardt, D. (2005). Phyllotaxis – a new chapter in an old tale about beauty and magic numbers. *Curr. Opin. Plant Biol.* **8**, 487-493.
Reinhart, B. J., Weinstein, E. G., Rhoades, M. W., Bartel, B. and Bartel, D. P. (2002). MicroRNAs in plants. *Genes Dev.* **16**, 1616-1626.
Rhoades, M. W., Reinhart, B. J., Lim, L. P., Burge, C. B., Bartel, B. and Bartel, D. P. (2002). Prediction of plant microRNA targets. *Cell* **110**, 513-520.
Rosso, M. G., Li, Y., Strizhov, N., Reiss, B., Dekker, K. and Weisshaar, B. (2003). An Arabidopsis thaliana T-DNA mutagenized population (GABI-Kat) for flanking sequence tag-based reverse genetics. *Plant Mol. Biol.* **53**, 247-259.
Schwab, R., Palatnik, J. F., Riester, M., Schommer, C., Schmid, M. and Weigel, D. (2005). Specific effects of microRNAs on the plant transcriptome. *Dev. Cell* **8**, 517-527.
Smyth, D. R., Bowman, J. L. and Meyerowitz, E. M. (1990). Early flower development in Arabidopsis. *Plant Cell* **2**, 755-767.
Sood, P., Krek, A., Zavolan, M., Macino, G. and Rajewsky, N. (2006). Cell-type-specific signatures of microRNAs on target mRNA expression. *Proc. Natl. Acad. Sci. USA* **103**, 2746-2751.
Stark, A., Brennecke, J., Bushati, N., Russell, R. B. and Cohen, S. M. (2005). Animal MicroRNAs confer robustness to gene expression and have a significant impact on 3′UTR evolution. *Cell* **123**, 1133-1146.
Takada, S., Hibara, K., Ishida, T. and Tasaka, M. (2001). The *CUP-SHAPED COTYLEDON1* gene of *Arabidopsis* regulates shoot apical meristem formation. *Development* **128**, 1127-1135.
Valencia-Sanchez, M. A., Liu, J., Hannon, G. J. and Parker, R. (2006). Control of translation and mRNA degradation by miRNAs and siRNAs. *Genes Dev.* **20**, 515-524.
Valoczi, A., Varallyay, E., Kauppinen, S., Burgyan, J. and Havelda, Z. (2006). Spatio-temporal accumulation of microRNAs is highly coordinated in developing plant tissues. *Plant J.* **47**, 140-151.
Vaucheret, H. (2006). Post-transcriptional small RNA pathways in plants: mechanisms and regulations. *Genes Dev.* **20**, 759-771.
Vaucheret, H., Mallory, A. C. and Bartel, D. P. (2006). AGO1 homeostasis entails coexpression of *MIR168* and *AGO1* and preferential stabilization of miR168 by AGO1. *Mol. Cell* **22**, 129-136.
Williams, L., Grigg, S. P., Xie, M., Christensen, S. and Fletcher, J. C. (2005). Regulation of Arabidopsis shoot apical meristem and lateral organ formation by microRNA miR166g and its AtHD-ZIP target genes. *Development* **132**, 3657-3668.